Nuclear Science & Technology Research Institute

Journal of Nuclear Research and Applications

Research Paper

Journal homepage: https://jonra.nstri.ir

Thermal Creep Behavior of Nanocrystalline Zr-Nb Binary Alloy at High Uniaxial Pressure in Atomic-Scale

M. R. Basaadat*

Physics and Accelerators Research School, Nuclear Science and Technology Research Institute, B. O. Box: 1439951113, Tehran, Iran.

(Received: 9 April 2024, Revised: 21 May 2024, Accepted: 28 May 2024)

A B S T R A C T

Zirconium (Zr) alloys with niobium are as an important structural material such as clad tubes, that are subjected to high-temperatures, pressures, and irradiation flux and their mechanical properties which can be changed in this process. In this study, the tensile creep behavior of these alloys has been investigated at high temperatures and pressures. The effect of grain size (GS) on the creep behavior of Zr-1%Nb alloy under different pressures and temperatures has been monitored using molecular dynamics approach. Accordingly, the deformation rate for the different creep stages (initial, steady-state, and tertiary stages) which is due to the production and diffusion of defects, has been explored. It has been shown that at high temperatures, the deformation rate of this alloy generally decreases with increasing GS. Furthermore, increasing the temperature and pressure results in a greater creep rate. Radial distribution function (RDF) and mean square displacement (MSD) have also been calculated for these cases to provide deeper insight into the creep behavior under tough condition.

***Keywords*:** Zr-1%Nb alloy, Molecular dynamics, Creep behavior, Grain size, High-temperature.

1. Introductions

Zirconium alloys have wide applications in the nuclear industry. They have high melting points, low cross-section for neutron capture, suitable corrosion resistance in water, and reliable mechanical properties and they have been used as structural material and cladding of water-cooled reactors [1–4]. Zircaloy-4 (Zr, Sn, Fe, O, Cr) is used in pressurized water reactors (PWR), Zircaloy-2 (Zr, Sn, O, Fe, Cr, Ni) in boiling water reactors (BWR) and, for Russian VVER's fuel rod geometryZr-1%Nb [5] which is claimed to have excellent post-irradiation ductility [6] is some of the common Zr-alloys.

Pure zirconium has a crystalline structure found in three main phases: α-phase with Hexagonal Close-Packed (HCP) structure at a

* Corresponding Author E-mail: mbasaadat@aeoi.org.ir

DOI: https://doi.org/10.24200/jonra.2024.1562.1118

temperature below 863 °C, β-phase with Body-Centered Cubic (BCC) structure at a temperature above 863 °C, and ω-phase with Hexagonal structure present under hydrostatic pressure [7,8] (Fig. 1).

Due to the importance of zirconium and its alloys' mechanical properties, one can find numerous experimental and ab-initio studies in the literature. For instance, Fisher and coworkers studied the elastic properties of single-crystal zirconium and the HCP to BCC transformation for group IV transition metals [9]. Phase transition and elastic constants of zirconium have been calculated by Yan-Jun et al. [10]. Temperature-dependent elastic constants for different elements and compositions have been studied by Varshni [11]. Weck and his coworkers calculated the mechanical properties of zirconium alloys and zirconium hydrides [12]. Furthermore, because molecular dynamics is a suitable tool to simulate the dynamics and evolution of materials, this method has also been used to study mechanical properties, and irradiation-dynamics of elements in various configurations, and the deformation mechanism in the different processes (The initial-, steady-state-, and tertiary stages) of creep process deformation. For example, the elastic properties of Zr-xNb alloy with defects and the effect of point defects on the properties of Zr and Zr-1%Nb structure have been studied by the author and his coworker with molecular dynamics approaches [13,14]. As an important mechanical performance parameter, there are experimental results on the creep behavior at high-temperature. Hayes and his coworkers consider the creep behavior of Zr-alloys experimentally for a limited pressure [15] and there are also other works on zirconium and other similar compositions in the literature [16–24].

It is important to apply the changes to the Zr-Nb alloy to give better stability and the for the designers of these structural materials. Therefore, mechanical properties such as creep deformation stages show the operability of this alloy for use in reactors. One of the important features of creep behavior calculations is the investigation of the structural dimensional instability in aggressive environments. For in-reactor service, the steady state creep stage is usually approached and it is rarely possible to reach the tertiary or unstable creep. When a fuel pellet is missing in the rod, there will be a high local creep and the material may enter to the tertiary creep stage [25] (see Fig. 2).

In this study, the deformation rates in different creep stages have been studied for Zr-1%Nb alloy. Furthermore, the temperature and uniaxial stress effects on creep behavior have been explored. In addition, the effect of GS on the creep performance of the alloy structure has been discussed. Then, the radial distribution function (RDF) for different temperatures has been studied to show the movement of atoms at various temperatures. Finally, the mean square distance (MSD) has been explored for different temperatures, pressures, and GSs of the Zr-1%Nb alloy. The paper is organized as follows. The second section is devoted to methods and computational details. The results have been explained and discussed in the third section. We conclude this study in the fourth section and, finally, the abbreviation section introduces the abbreviations of the words used in this article.

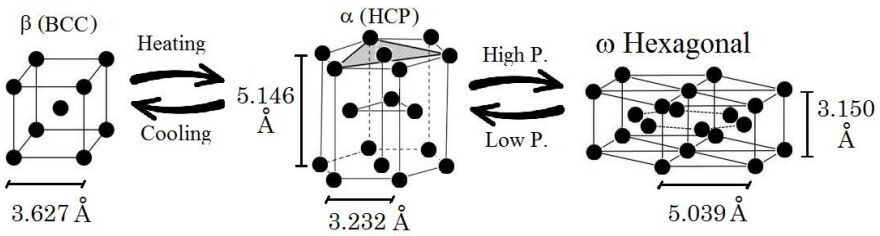

Fig. 1. Different zirconium phases.

2. Methods and computational details

Three nanocrystalline Zr-1%Nb alloys have been generated with different GS values of 10, 30, and 50 grains, and with 144761, 144338, and 144311 atoms in each nanocrystalline respectively by Atomsk [26]. The geometric structure is a cube of HCP grains with 15.0 nm× 15.0 nm× 15.0 nm in each direction and various grains orientations (Fig. 3). The volume of each grain is obtained as (V /N) where V is the total volume and N is the number of grains. In the same way, the grain sizesare the cubic side of grain and are 4.1 nm, 4.8 nm, and 6.7 nm in these three configurations. Each grain is distinguished by different colors and fragments. In addition, the Voronoi algorithm [27] has been used to produce these nanocrystallines. The periodic boundary condition was used in all directions.

All of the simulations have been done by Large-scale Atomic/Molecular Massively Parallel Simulator (LAMMPS) [28], a popular package for consideration of molecular dynamics evolution of the system classically. A Zr-Nb binary interatomic potential [29] has been used for the system in the angular-dependent potential (ADP) format. It reproduces reasonably accurate results for the thermal and mechanical properties of pure elements and binary composition alloys. It is also reliable for studing different defects in this structure and usesthe Embedded Atom Method (EAM) potential. The dipole and quadrupole distortions terms are included in this potential. In addition, the time-step was set to 1 fs.Furthermore, the visual software VMD [30] was used for structural post processing analysis.

First, the Zr-1%Nb nanocrystalline wasfully optimized, and then the creep process simulations were performed using the Nose-Hoover non-Hamiltonian equations of motion. These produces the positions and velocities on the isothermal-isobaric (NPT) ensemble as mentioned in the Shinoda et. al. [31], where only constant uniaxial stress is applied in the Z direction, and no other stress is available in the other directions. The creep simulations were performed for 100 Ps at high temperatures to provide deep insights with respect to the crystal structure evolution. RDF was calculated to determine the degree of non-crystallization during the high-temperature creep process. MSD is a substantial parameter for analyzingthe atomic diffusion coefficient of the system. Hence, MSD was calculated in the next part using the method of Meraj et. al. [32] method:

$$MSD(t) = \langle r^2(t) \rangle = \langle \frac{1}{N} (\sum_{i=0}^{N} (r_i(t) - r_i(0))^2) \rangle \quad (1)$$

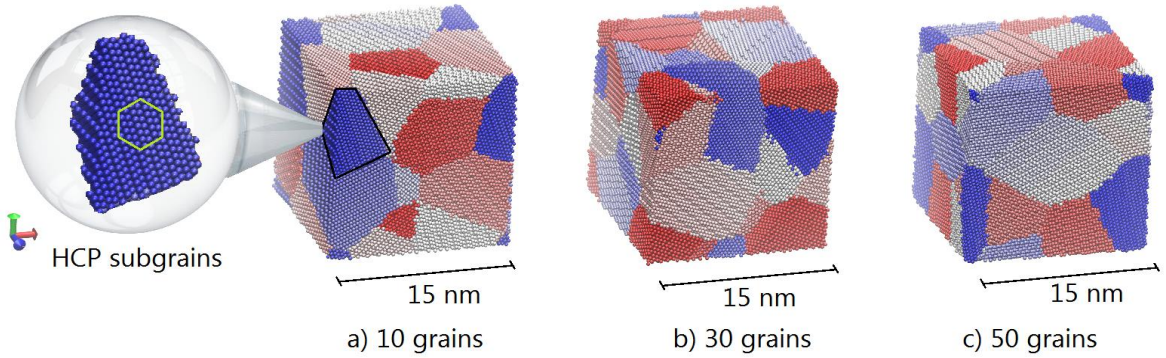

a) 10 grains b) 30 grains c) 50 grains

Fig. 3. a) 6.7 nm GS, b) 4.8 nm GS and c) 4.1 nm GS of the nanocrystalline of Zr-1%Nb alloy.

3. Results and discussion

3.1. Lattice constants and defect formation energies verification

First, the interatomic potential should be evaluated against available experimental results. For this purpose, the lattice parameters of single crystal HCP zirconium were obtained as 3.188, 5.206 Å in X- and Z-directions, respectively, which are in accordance with experimental vaalues. (3.232, 5.149 Å [33]). Because the most dominant events in the creep process are the production and annihilation of vacancies and self-interstitials, either as point defects or different forms of extended defects, the formation energy of these defects is a prominent characteristics in these calculations. Thus, the verification of vacancy and selfinterstitial formation energies with experimental data and other calculations is very important. For this purpose, these quantities for single crystal zirconium structure were obtained as 1.90, and 2.76 eV, respectively, which can be compared with experimental values (> 1 eV [34]) and DFT results (2.75 eV [35]). It can be generally concluded that this interatomic potential provides reliable results in our calculations.

3.2. Deformation rate under uniaxial stress

For the purpose of creep molecular dynamics (MD) simulations, it is important to note that that time and size scales limit these calculations when compared with experimental results. Although the stress and strain levels obtained from MD simulations are for small volumes and short time scales and may be much higher than actual values, this stress and strain can be considered as local stress. The key point here is that creep is a time-related phenomenon, and MD simulations can be performedfor the creep phenomenon and different strain rates beyond the timescale. Moreover, the characteristics of creep simulated by MD are consistent with the true three stages of creep:: initial, steady-state, and tertiary creep. Furthermore, in the case of grain size, the normal mean grain size of Zr alloys is approximately 5 μm [22] but well-defined subgrain boundaries can form during the creep process [36]. Thus, it is rational to use MD for the study of the creep deformation behavior [37].

In this section, different high uniaxial stresses (from 0.8 GPa to 1.2 GPa) have been applied to the nanocrystalline Zr-1%Nb alloy with different grain sizes and in various temperatures (600, 900, and 1200 K). The creep deformation process is shown in fig. 4. Green, pink and black colors show the 0.8, 1.0, and 1.2 GPa pressure respectively in each plot. As mentioned, three creep stages can be found in Fig. 4: the initial creep, the steady-state, and the tertiary creep stages. These curves can be divided into two parts; at low temperatures (600 K) most of the deformation rates do not include the tertiary stage. However, the creep behavior of the nanocrystalline material is mostly in the tertiary form at higher temperatures. As the temperature increases, the vibration amplitude of the atoms in the alloy structure increases so that some of the atoms may overcome the adjacent barrier in presence of a pressure gradient, and increases the internal diffusion of defects. These creep processes occur at high pressure and for this reason, it is expected that for increasing the temperature, the steady-state creep stage is going to be fades away. In other words, increasing the temperature gradually decreases the steady-state time duration stage and speeds up the tertiary creep stage. Based on this, the structure may undergo to necking or even rupture for high pressure and temperature. One important point is that these calculations have been done near the interface of α/β-phase boundaries of Zr-1%Nb alloy and sometimes this alloy can be locally found in α+β-phase and that is why deformation rate for 1200 K and under the high uniaxial stress shows a little different treatment from the general trends.

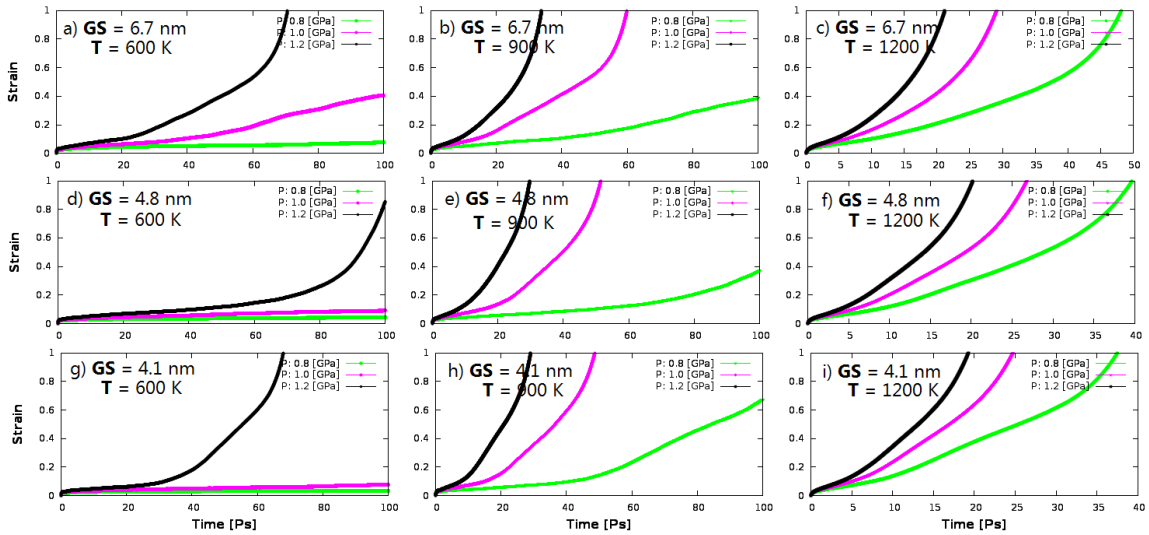

Fig. 4. The deformation rate of Zr-1%Nb alloy for different grain sizes and temperatures and uniaxial stresses. a) 6.7 nm at 600 K; b) 6.7 nm at 900 K; c) 6.7 nm at 1200 K; d) 4.8 nm at 600 K; e) 4.8 nm at 900 K; f) 4.8 nm at 1200 K; g) 4.1 nm at 600 K; h) 4.1 nm at 900 K; and i) 4.1 nm at 1200 K.

As far as we know, most of the experimental results for the creep behavior of Zralloys have been conducted for low pressures and it is shown that here for high pressure the accelerated creep stage would be a dominant phenomenon. Increasing the pressure increases the equilibrium vacancy concentration and it may cause a faster creep process as can be seen generally in fig. 4. It can be seen that, for example, for temperature 900 K increasing GS reduces the creep rate. Although this process is done in an aggressive environment and is not completely identical for all temperatures and pressures, the general statement about GS effects on the creep process is that this process accelerates with the decrease of GS and thus shortened the creep life of Zr-1%Nb alloy. Decreasing the GS, indeed, causes an increase in the surface to-volume ratio, and equivalently it would increase the grain boundary. Since the grain boundary is the best place to form dislocations and vacancies [38,39] as a sink or source, increasing the grain boundary provides a convenient path for defect diffusion. Thus, the probability of sliding dislocations or diffusion of other defects would be increases, and it is more probable to deform the structure and the creep process will speed up.

3.3. Radial distribution function and crystal structure evolution

The radial distribution function is a measure of how the environmental density of a materialvaries with distance from a particle point. This quantity is demonstrated in Fig. 4 for 4.1 nm grain size during the creep process under 0.8 GPa pressure as a typical RDF for these creep simulations. Different temperatures and time steps (from a to d) have been determined and the disordering effects can be observed during the creep deformation process. The grain boundaries increase when the temperature rises and it increasesthe disorder of the structure and atom vibrations may cause amorphization of the atoms on the edge of the grains. At the same time, increasing the disorder in the grain interior may lead to the phase transition of the structure from α to β and it is more probable for defects, especially dislocations, to move and diffuse and the creep deformation stages can speed up in this case. On the other hand, the RDF spikes, which are

defined as the probability of finding identical particles as a function of distance, become broader with increasing temperature. It means that the particles experience increased vibrations and the structure disorders have increased with temperature. In addition, because of the thermal motion of the particles, the third and fourth peaks which are very near together at 600 K, merge into one peak at 900, and 1200 K, and this process is repeated for the rest of the graph. The tailing peaks have gradually disappeared, and it shows the amorphization treatment for high temperatures. Moreover, when the RDF graphs begin to separate from each other during the time, it means that the probability of finding the particles is significantly altered, and the structure may not be stable and the creep deformation may progress to necking or rupture. In this case, there is no separation for temperatures 600 and 900 K, but it can be observed a small separation for the temperature 1200 K at 20 Ps and this separation is greater for 50 Ps. The results of the creep process for this case (Fig. 4-g) are in accordance with the RDF graph because the creep behavior of the structure for both lowest temperatures is in the steady-state stage and it is in the tertiary stage at 1200 K.

3.4. Mean square distance

Mean square distance (MSD) is one of the useful quantities to improve the creep behavior understanding process. As mentioned in the second section (eq. 1), this factor is a measure of the atomic displacement from their initial point in the structure. In other words, the time evolution path of atomic displacements has been quantitatively represented by MSD. The atomic displacements lead to defect production such as vacancies, self-interstitials (SI), different types of dislocations, and extended defects like voids and stacking faults. Defect production can, however, diffuse in the structure in the presence of a pressure gradient and it may lead to the creep deformation. Regardless of how complicated the defect-type evolution process is, the high value of MSD may be interpreted as the creep process in the structure. It can be seen in Fig. 5 that the trends of all graphs are the same as creep deformation (Fig. 4). It means that the atomic displacements or defect diffusions have a vital role in the creep mechanism. It can be stated that the decrease of GS may lead to an increase in the diffusion rate of atoms. In addition, this atomic diffusion rate increases with temperature and pressure. As MSD increases, the extent of amorphization of the grains increases and more vacancies and SIs are produced so that the atomic diffusion increases. It can be concluded that diffusion creep is a dominant factor in the creep mechanism of the Zr-1%Nb alloy structure.

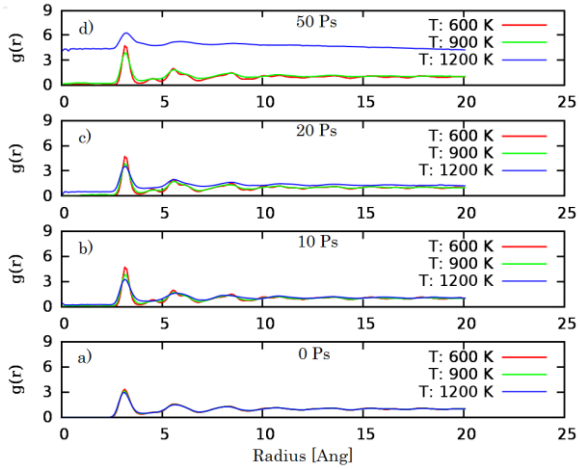

Fig. 5. Different timesteps for radial distribution function with 4.1 nm grain at the 0.8 GPa stress at different temperatures.

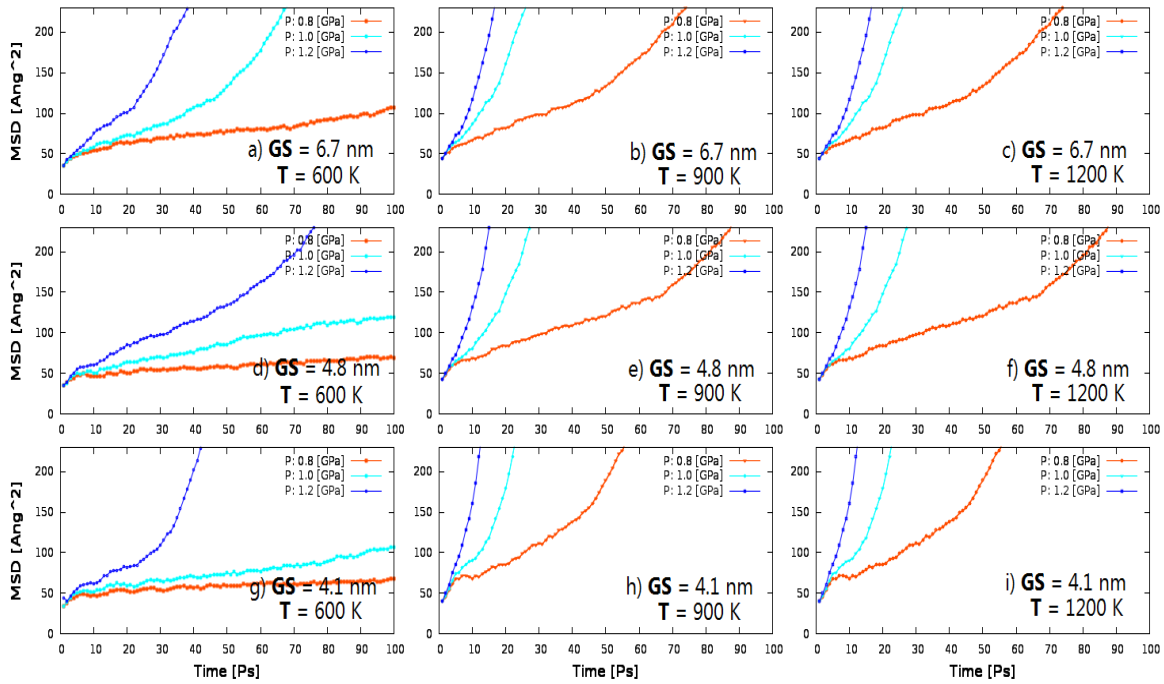

Fig. 6. Time evolution of MSD for the Zr-1%Nb alloy with different grain sizes, temperatures and stresses: (a) 6.7 nm at 600 K; (b) 6.7 nm at 900 K; (c) 6.7 nm at 1200 K; (d) 4.8 nm at 600 K; (e) 4.8 nm at 900 K; (f) 4.8 nm at 1200 K; (g) 4.1 nm at 600 K; (h) 4.1 nm at 900 K; and (i) 4.1 nm at 1200 K.

4. Conclusion

The creep behavior of materials that are used in the nuclear industry is a prominent subject that has been considered for many years and due to the necessity of the use of simulations, molecular dynamics is a powerful tool for analysis of this phenomenon. In this study, we discussed the high-temperature, high-pressure, and grain size effects during the creep deformation process and analyzed the results. It was shown that increasing the temperature and pressure led to an increase in the creep deformation rate. As we discussed the system under high pressure and temperature, many of the simulated structures were in the tertiary creep stage and they should be unstable. As discussed, the structure of fuel cladding is not stable at high pressure and low pressure, the structure of fuel cladding is in the steady-state stage, but there was an exception for missing fuel pellets in the rod that may lead to high local creep and the system may be in the tertiary creep stage. The radial distribution function was calculated and it was shown that this quantity broadens as the temperature rises.. The atoms actually may have more vibrations with temperature which leads to atomic disorder and may affect the creep process. Finally, the mean square distance was calculated and it was shown that the increase in MSD is a consequence of the increase in the deformation rate. Furthermore, atomic diffusion is a dominant process during the creep phenomenon.

Nomenclature

GS	Grain Size
HCP	Hexagonal Close-packed
BCC	Body-Centered Cubic
RDF	Radial Distribution Function
MSD	Mean Square Distance
ADP	Angular Dependent Potential
SI	Self-Interstitial

Conflict of interest

The authors declare no potential conflict of interest regarding the publication of this work.

References

[1] Rickover HG, Geiger LD, Lustman B. History of the development of zirconium alloys for use in nuclear reactors. Energy Research and Development Administration, Washington, DC (USA). Div. of Naval Reactors; 1975 Mar 21.

[2] Lustman B, Kerze F, Straumanis ME. The metallurgy of zirconium. Journal of The Electrochemical Society. 1957 Dec 1;104(12):254Ca.

[3] Adamson R, Cox B, Garzarolli F, Strasser A, Rudling P, Wikmark G. ZIRAT-10 Special Topics Report. Impact of Irradiation on Material Performance, ANT International, Sweden. 2005 Oct.

[4] Bell BD, Murphy ST, Burr PA, Comstock RJ, Partezana JM, Grimes RW, Wenman MR. The influence of alloying elements on the corrosion of Zr alloys. Corrosion Science. 2016 Apr 1;105:36-43.

[5] Lemaignan C, Motta AT. Zirconium alloys in nuclear applications. Materials science and technology. 2006 Sep 15.

[6] Northwood DO. The development and applications of zirconium alloys. Materials & design. 1985 Apr 1;6(2):58-70.

[7] Kharchenko VO, Kharchenko DO. Ab-initio calculations for structural properties of Zr-Nb alloys. arXiv preprint arXiv:1206.7035. 2012 Jun 29.

[8] Van Groenigen JW, Lubbers IM, Vos HM, Brown GG, De Deyn GB, Van Groenigen KJ. Earthworms increase plant production: a meta-analysis. Scientific reports. 2014 Sep 15;4(1):6365.

[9] Fisher ES, Renken CJ. Single-crystal elastic moduli and the hcp→ bcc transformation in Ti, Zr, and Hf. Physical review. 1964 Jul 20;135(2A):A482.

[10] Hao YJ, Zhang L, Chen XR, Li YH, He HL. Phase transition and elastic constants of zirconium from first-principles calculations. Journal of Physics: Condensed Matter. 2008 May 9;20(23):235230.

[11] Varshni YP. Temperature dependence of the elastic constants. Physical Review B. 1970 Nov 15;2(10):3952.

[12] Weck PF, Kim E, Tikare V, Mitchell JA. Mechanical properties of zirconium alloys and zirconium hydrides predicted from density functional perturbation theory. Dalton Transactions. 2015;44(43):18769-79.

[13] Basaadat MR, Payami M. Elastic stiffness tensors of Zr–x Nb alloy in the presence of defects: A molecular dynamics study. International Journal of Modern Physics C. 2020 Feb 24;31(02):2050028.

[14] Payami Shabestar M, Basaadat MR. The study of the properties of point defects in pure-Zr and Zr-1% Nb alloy using density-functional theory and atomic simulation. Iranian Journal of Physics Research. 2020 May 21;20(1):57-64.

[15] Hayes TA, Kassner ME. Creep of zirconium and zirconium alloys. Metallurgical and Materials Transactions A. 2006 Aug;37:2389-96.

[16] Ashkenazi J, Dacorogna M, Peter M, Talmor Y, Walker E, Steinemann S. Elastic constants in Nb-Zr alloys from zero temperature to the melting point: Experiment and theory. Physical Review B. 1978 Oct 15;18(8):4120.

[17] Bolef DI. Elastic constants of single crystals of the bcc transition elements V, Nb, and Ta. Journal of Applied Physics. 1961 Jan 1;32(1):100-5.

[18] Hayes D. J., and Brotzen F. R., Journal of Applied Physics, 45(4) (1974), pp.1721–1725.

[19] Fast L, Wills JM, Johansson B, Eriksson O. Elastic constants of hexagonal transition metals: Theory. Physical Review B. 1995 Jun 15;51(24):17431.

[20] Al-Zoubi N, Schönecker S, Li X, Li W, Johansson B, Vitos L. Elastic properties of 4d transition metal alloys: Values and trends. Computational materials science. 2019 Mar 1;159:273-80.

[21] Pal S, Meraj M, Deng C. Effect of Zr addition on creep properties of ultra-fine grained nanocrystalline Ni studied by molecular dynamics simulations. Computational Materials Science. 2017 Jan 1;126:382-92.

[22] Kaddour D, Frechinet S, Gourgues AF, Brachet JC, Portier L, Pineau A. Experimental determination of creep properties of zirconium alloys together with phase transformation. Scripta materialia. 2004 Sep 1;51(6):515-9.

[23] Kaddour D, Frechinet S, Gourgues AF, Brachet JC, Portier L, Pineau A. Experimental determination of creep properties of zirconium alloys together with phase transformation. Scripta materialia. 2004 Sep 1;51(6):515-9.

[24] Adamson RB, Coleman CE, Griffiths M. Irradiation creep and growth of zirconium alloys: A critical review. Journal of Nuclear Materials. 2019 Aug 1;521:167-244.

[25] Franklin DG, Adamson RB. Implications of Zircaloy creep and growth to light water reactor performance. Journal of Nuclear Materials. 1988 Oct 1;159:12-21.

[26] Hirel P. Atomsk: A tool for manipulating and converting atomic data files. Computer Physics Communications. 2015 Dec 1;197:212-9.

[27] Chen D. Structural modeling of nanocrystalline materials. Computational materials science. 1995 Jan 1;3(3):327-33.

[28] Plimpton S. Fast parallel algorithms for short-range molecular dynamics. Journal of computational physics. 1995 Mar 1;117(1):1-9.

[29] Smirnova DE, Starikov SV. An interatomic potential for simulation of Zr-Nb system.

Computational Materials Science. 2017 Mar 1;129:259-72.
[30] Humphrey W, Dalke A, Schulten K. VMD: visual molecular dynamics. Journal of molecular graphics. 1996 Feb 1;14(1):33-8.
[31] Shinoda W, Shiga M, Mikami M. Rapid estimation of elastic constants by molecular dynamics simulation under constant stress. Physical Review B. 2004 Apr 7;69(13):134103.
[32] Meraj M, Pal S. Creep Behavior Study of Join of Nano Crystalline Stainless Steel and Nanocrystalline Nickel Using Molecular Dynamics Simulation.
[33] Swanson ML. Low temperature recovery of deformed zirconium. Canadian Journal of Physics. 1966 Dec 1;44(12):3241-57.
[34] Samolyuk GD, Golubov SI, Osetsky YN, Stoller RE. Self-interstitial configurations in hcp Zr: a first principles analysis. Philosophical magazine letters. 2013 Feb 1;93(2):93-100.
[35] Wolfer WG. Fundamental properties of defects in metals. Comprehensive nuclear materials. 2012 Jan 1;1:1-45.
[36] Kassner ME. Fundamentals of creep in metals and alloys. Butterworth-Heinemann; 2015 Jan 6.
[37] Zhao F, Zhang J, He C, Zhang Y, Gao X, Xie L. Molecular dynamics simulation on creep behavior of nanocrystalline TiAl alloy. Nanomaterials. 2020 Aug 28;10(9):1693.
[38] Meyers MA, Mishra A, Benson DJ. Mechanical properties of nanocrystalline materials. Progress in materials science. 2006 May 1;51(4):427-556.
[39] Ashby MF, Jones DR. Engineering materials 1: an introduction to properties, applications and design. Elsevier; 2012.

How to cite this article

M. R. Basaadat, *Thermal Creep Behavior of Nanocrystalline Zr-Nb Binary Alloy at High Uniaxial Pressure in Atomic-Scale*, Journal of Nuclear Research and Applications (JONRA) Volume 4 Number 2 Spring (2024) 20-28. **URL**: https://jonra.nstri.ir/article_1652.html, **DOI**: https://doi.org/10.24200/jonra.2024.1562.1118.